

# Electrical Characterization Of Lead-Free (1-X)(Ba<sub>0.90</sub>Sr<sub>0.10</sub>)(Zr<sub>0.20</sub>Ti<sub>0.80</sub>)O<sub>3</sub>-Xnanbo<sub>3</sub> Relaxor Ceramics For Capacitor Application

Md Jahidul Haque<sup>1</sup>, Md Shamimur Rahman<sup>2</sup>

<sup>1</sup>Student, Department of Glass & Ceramic Engineering, Rajshahi University of Engineering & Technology (RUET), Rajshahi-6204, Bangladesh.

<sup>2</sup>Professor, Department of Glass & Ceramic Engineering, Rajshahi University of Engineering & Technology (RUET), Rajshahi-6204, Bangladesh.

Corresponding Author: [mjh.ruet26@gmail.com](mailto:mjh.ruet26@gmail.com)

**Abstract:** - In the present work, (1-x)(Ba<sub>0.90</sub>Sr<sub>0.10</sub>)(Zr<sub>0.20</sub>Ti<sub>0.80</sub>)O<sub>3</sub>-xNaNbO<sub>3</sub> (x = 0.00, 0.05, 0.10, 0.15, 0.20) based relaxor ceramics were prepared through solid-state reaction route. Morphological and electrical characterizations were performed. Polygonal-type grains were observed. 10% NN-based composition exhibited the highest average grain size value (~740.96 nm). EDX analysis ensured the presence of Ba, Sr, Zr, Ti, Na, and Nb within the compositions. 10% NN-based composition showed a better Q-factor curve compared to others. It also showed the highest resistivity value. All of the compositions showed a strong relationship between the electrical properties with frequency and ensured their application in energy storage-based electronic devices.

**Key Words:** Relaxor ceramics, EDX, Q-factor, Resistivity.

## I. INTRODUCTION

Due to the high rate of consumption of fossil fuels, it is time to think of another mechanism that can store significant amounts of energy [1]. Capacitors are considered as such devices for satisfying the purpose. Capacitors hold a great position in modern technology [2,3]. In capacitors, mainly four types of dielectric materials are used such as linear dielectrics, classical ferroelectrics, anti-ferroelectrics, and relaxor dielectrics [4]. The first three show some issues regarding the breakdown strength and their successive dielectric properties. However, the fourth one solves the issues mentioned previously [5–7]. Relaxor ceramics are a broad class of materials that shows a significant change in dielectric constant and loss concerning frequency.

The first relaxor ceramic was lead magnesium niobate (PbMg<sub>1/3</sub>Nb<sub>2/3</sub>O<sub>3</sub>) or PMN as developed in the early 1950s.

Some other relaxor ceramics are lead zinc niobate (PZN), lead iron niobate (PFN), lead magnesium niobate with lead titanate (PMN-PT), and so on. Relaxor ceramics contains perovskite crystal structure. But a problem arises for compositions that contain Pb and Nb. These materials pass through a transition from perovskite to pyrochlore structure. Pyrochlore holds a paraelectric crystal structure that has a very low dielectric constant of almost 130. Barium Titanate (BaTiO<sub>3</sub>) or BT has a high dielectric constant and low dielectric loss, but low breakdown strength [8,9]. This problem can be solved by substituting the A-site and B-site cations with iso-valent cations. Again, sodium niobate (NaNbO<sub>3</sub>) or NN shows a phase transition between anti-ferroelectric to ferroelectric) and it can be solved by combining it with a solid solution, mainly the formation of a composite [10,11].

In the present work, BT was doped with Sr<sup>2+</sup> (for A-site) and Zr<sup>4+</sup> (for B-site) [12–14]. Again, BT is not a relaxor ceramic in this form. So, the NN phase was combined at different percentages of 0, 5, 10, 15, and 20%. The physical, morphological, and electrical characterization was performed for ensuring their relaxor characteristics.

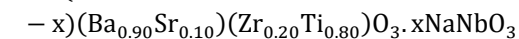
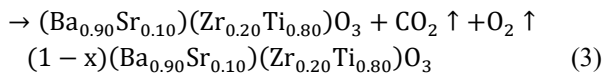
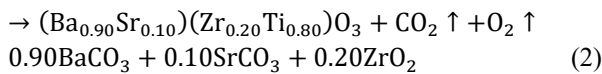
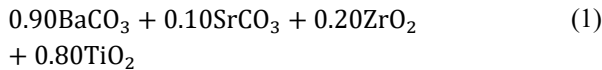
Manuscript revised April 06, 2023; accepted April 07, 2023. Date of publication April 09, 2023.

This paper available online at [www.ijprse.com](http://www.ijprse.com)

ISSN (Online): 2582-7898; SJIF: 5.59

## II. METHODOLOGY

In this experiment,  $(1-x)(\text{Ba}_{0.90}\text{Sr}_{0.10})(\text{Zr}_{0.20}\text{Ti}_{0.80})\text{O}_3 \cdot x\text{NaNbO}_3$  ( $x = 0.00, 0.05, 0.10, 0.15, 0.20$ ) based relaxor ceramics were prepared by solid-state sintering method. As the composition held two different phases. The phases were prepared individually. At first for  $(\text{Ba}_{0.90}\text{Sr}_{0.10})(\text{Zr}_{0.20}\text{Ti}_{0.80})\text{O}_3$  phase the starting raw materials included  $\text{BaCO}_3$ ,  $\text{SrCO}_3$ ,  $\text{ZrO}_2$ , and  $\text{TiO}_2$ . The raw materials were weighed maintaining the stoichiometric ratio, mixed and ball milled for 15 h. After milling the slurry was dried at  $80^\circ\text{C}$  and then calcined at  $1050^\circ\text{C}$  for 4 h. Finally, the calcined powder was sintered at  $1225^\circ\text{C}$  for 4 h. Now, for the second phase of  $\text{NaNbO}_3$ , the aforementioned steps were also followed. Here, the starting raw materials included  $\text{Na}_2\text{CO}_3$  and  $\text{Nb}_2\text{O}_5$ . The dried powder was calcined at  $870^\circ\text{C}$  for 3 h and then sintered at  $1125^\circ\text{C}$  for 3 h. Both phases were then weighed, mixed (based on different compositions) and ball milled for 15 h. At last, the powders were transformed into pellets using a press plate (having a pressure of 3 tons) and annealed at  $900^\circ\text{C}$  for 2 h. The bulk density of the specimens was measured using the dry weight and volume of the samples. The synthesized relaxor ceramics were then characterized by a Scanning Electron Microscope (analyzing surface morphology), Energy Dispersive X-ray Spectroscopy (analyzing inherent elemental composition), and finally Impedance Analyzer (analyzing Q-factor and resistivity against frequency). However, the compositions are designated as BSZT, 95%BSZT-5%NN, 90%BSZT-10%NN, 85%BSZT-15%NN, 80%BSZT-20%NN for 0, 5, 10, 15, and 20% NN incorporation. The successive reactions during sintering are given below:



Where,  $x = 0.00, 0.05, 0.10, 0.15$  and  $0.20$

## III. RESULTS AND DISCUSSION

### 3.1 Bulk Density

According to the American Society for Testing and Materials (ASTM-C29/C29M), the bulk density ( $\rho = m/v$ ) was measured. The values are tabulated in Table 1. Here, the density values of the composites are lower compared to 0% NN-based composition. It is mainly caused due to the lower molecular weight of NN (163.89 g/mol) than BT's (233.19 g/mol).

Table.1. Physical parameters of the compositions.

Composition	Bulk Density (g/cm <sup>3</sup> )	Average grain size (nm)
BSZT	3.54	710.08
95%BSZT-5%NN	3.52	711.89
90%BSZT-10%NN	3.53	740.96
85%BSZT-15%NN	2.89	685.62
80%BSZT-20%NN	2.29	593.19

### 3.2 Morphological analysis

Fig. 1 shows the scanning electron micrographs of the synthesized relaxor ceramics. All of the compositions show polygonal-type grain arrangement. Composition of 0, 5, and 10% NN display significant grain arrangement. Whereas, the grains are not identical for the composition of 15 and 20% NN. The average grain size was measured by the linear intercept method using ImageJ software.

The values are summarized in Table 1. The average grain size increases up to 10% NN-based composition. It is due to the difference in the densification temperature between BSZT and NN phases. The following decrement pattern is caused due to the grain confinement effect. As the NN phase increases, it takes place around the grains of the BSZT phase and restricts the diffusion mechanism as well as the grain growth of the BSZT phase.

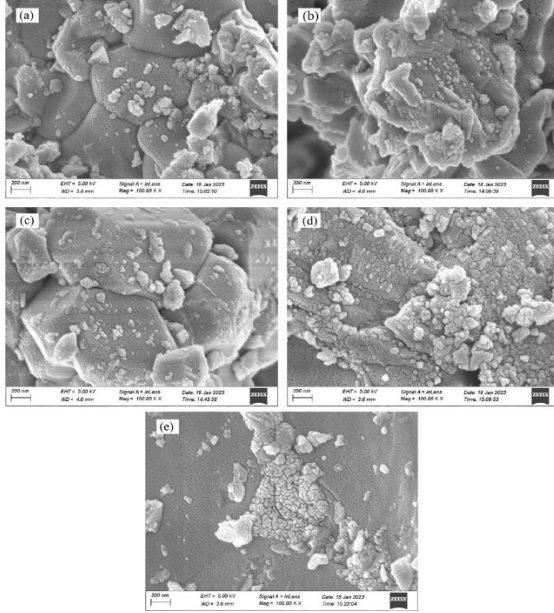


Fig.1. Scanning electron micrographs of (a) BSZT, (b) 95%BSZT-5%NN, (c) 90%BSZT-10%NN, (d) 85%BSZT-15%NN and (e) 80%BSZT-20%NN ceramics.

### 3.3 EDX analysis

Fig. 2 shows the Energy Dispersive X-ray Spectroscopy curves of the synthesized relaxor ceramics. It provides information on the elemental composition. All elements show their corresponding identical peaks. Here, the peaks of Ba, Sr, Zr, Ti, Na, and Nb peaks are observed. This ensures the presence of the elements within the compositions.

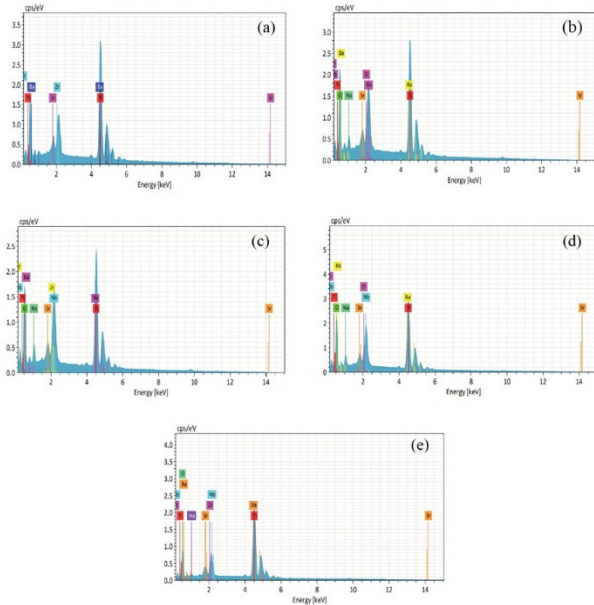


Fig.2. EDX curves of (a) BSZT, (b) 95%BSZT-5%NN, (c) 90%BSZT-10%NN, (d) 85%BSZT-15%NN, and (e) 80%BSZT-20%NN relaxor ceramics.

### 3.4 Electrical analysis

#### 3.4.1 Quality factor

Fig. 3 shows the quality factor (Q-factor) curves of (1-x)BSZT-xNN relaxor ceramics. It denotes a dimensionless parameter that describes how much an electrical system is underdamped under working conditions. It also determines the effectiveness of capacitors based on their losses and the bandwidth of the resonator. The Q-factor exhibits energy losses because of the amount of energy stored within the system. Generally, the larger the Q-factor, the lower the loss and consequently, passing through a low percentage of damping. Often, the loss of the Q-factor is triggered due to the resistance to the system. The Q factor of a capacitor is given below:

$$Q_c = \frac{-X_c}{R_c} = \frac{1}{\omega_0 C R_c} \quad (4)$$

Where,  $\omega_0$  is the resonance frequency, C is capacitance,  $X_c$  is inductive reactance and  $R_c$  is the resistance of the capacitance. From the curves it is observed that 90%BSZT-10%NN and 95%BSZT-15%NN show increased Q factor values, ensuring excessive oscillation concerning frequency. On the contrary, other compositions show lower Q-factor values. So, these systems remain damped during operational condition.

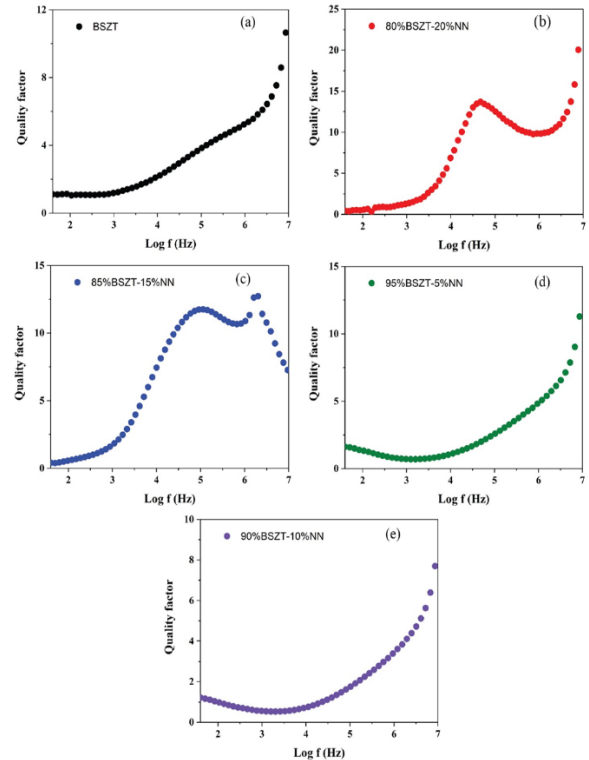
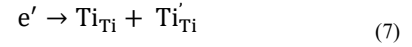
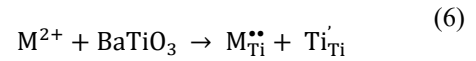
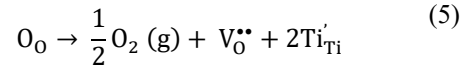


Fig.3. Q factor vs log frequency curves of the relaxor ceramics.

### 3.4.2 Resistivity

Fig. 4 shows the frequency-dependent resistivity curves of the relaxor ceramics. At the starting frequency, all of the compositions show higher resistivity. But, with increasing frequency, the resistivity decreases and finally becomes flattened at a higher frequency. There is a relation between the average grain size and the resistivity. If the grain size becomes larger, the surface area decreases which in turn reduces the area of the grain boundary. The grain boundary acts as the source of imperfection that contains ions, charges, foreign inclusions, and so on. These imperfections participate in the charge movement mechanism among neighboring sites and consequently reduce the resistivity and induce ac conductivity. 90%BSZT-10%NN holds the highest average grain size value and so it shows better resistivity compared to other relaxor ceramics. 95%BSZT-5%NN and 85%BSZT-15%NN also show satisfactory resistivity, whereas 80%BSZT-20%NN show to a low value of resistivity. The lower value of resistivity ensures the presence of extensive ac conductivity within the system. This mainly occurred due to the polaron hopping mechanism. Usually, a polaron consists of a charge and its surrounding electric field. The charge is mainly generated by oxygen vacancy through atmospheric reduction or donor doping, according to the following reactions:



Often it is believed that the dielectric constant shows a proportional relationship with resistivity. So, 90%BSZT-10%NN is believed to have the highest dielectric constant based on this theory. The resistivity values of all the compositions at the frequency of 1000 Hz are summarized in Table 2.

Table.2. Resistivity values of the relaxor ceramics at 1000 Hz.

Composition	Resistivity ( $\Omega, \times 10^6$ )
BSZT	13.93
95%BSZT-5%NN	36.12
90%BSZT-10%NN	115.24
85%BSZT-15%NN	15.58
80%BSZT-20%NN	3.03

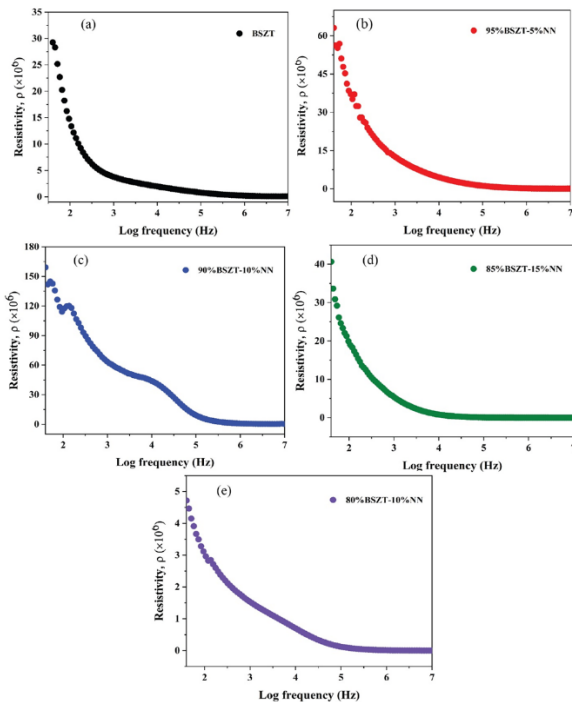


Fig.4. Resistivity vs log frequency curves of the synthesized compositions.

## IV. CONCLUSION

(1-x) (Ba<sub>0.90</sub>Sr<sub>0.10</sub>) (Zr<sub>0.20</sub>Ti<sub>0.80</sub>) O<sub>3-x</sub>NaNbO<sub>3</sub> (x = 0.00, 0.05, 0.10, 0.15, 0.20) relaxor ceramics were synthesized. The method was solid-state sintering. Physical, morphological, and electrical properties were analyzed. The bulk density of composites was lower compared to the base composition. The grain arrangement was a polygonal type. EDX ensures the presence of doped and substitute elements. Although, the composition of 0%, 15%, and 20% NN were underdamped at working conditions. 5% and 10% NN showed low damping conditions. 10% NN-based composition derived the highest resistivity value against ac conductivity. Other compositions

also showed satisfactory values except for 20% NN-based composition. However, based on their responses, it can be concluded that these compositions can be effectively used as a relaxor dielectric material for capacitor applications.

*Acknowledgment:*

I, as a corresponding author, show my gratitude to members of the Department of Glass & Ceramic Engineering, Rajshahi University of Engineering & Technology for their cordial support during performing this research work.

**REFERENCES**

- [1]. X. Huang, B. Sun, Y. Zhu, S. Li, P. Jiang, High-k polymer nanocomposites with 1D filler for dielectric and energy storage applications, *Prog. Mater. Sci.* 100 (2019) 187–225.
- [2]. L. Yang, X. Kong, F. Li, H. Hao, Z. Cheng, H. Liu, J.F. Li, S. Zhang, Perovskite lead-free dielectrics for energy storage applications, *Prog. Mater. Sci.* 102 (2019) 72–108.
- [3]. S. Liu, B. Shen, H. Hao, J. Zhai, Glass-ceramic dielectric materials with high energy density and ultra-fast discharge speed for high power energy storage applications, *J. Mater. Chem. C* 7 (2019) 15118–15135.
- [4]. Y.L. and F.L.W. Aditya Jain, Y. G. Wang, N. Wang, Synergetic effect of BiYb<sub>0.9</sub>Sc<sub>0.1</sub>O<sub>3</sub> substitution on the energy storage performance of Ba<sub>0.90</sub>Sr<sub>0.10</sub>Ti<sub>0.90</sub>Zr<sub>0.10</sub>O<sub>3</sub> ferroelectric ceramic, *J. Phys. D: Appl. Phys.* 55 (2020).
- [5]. S.B. Li, L.M. Zhang, C.B. Wang, X. Ji, Q. Shen, Structural, dielectric and ferroelectric properties of lead-free Ba<sub>0.85</sub>Ca<sub>0.15</sub>Zr<sub>0.10</sub>Ti<sub>0.90</sub>O<sub>3</sub> ceramics prepared by Plasma Activated Sintering, *Ceram. Int.* 42 (2016) 18585–18591.
- [6]. A. Jain, A.K. Panwar, A.K. Jha, Significant improvement in morphological, dielectric, ferroelectric and piezoelectric characteristics of Ba<sub>0.9</sub>Sr<sub>0.1</sub>Ti<sub>0.9</sub>Zr<sub>0.1</sub>O<sub>3</sub>–BaNb<sub>2</sub>O<sub>6</sub> nanocomposites, *J. Mater. Sci. Mater. Electron.* 29 (2018) 19086–19098.
- [7]. A. Jain, Y.G. Wang, N. Wang, Y. Li, F.L. Wang, Existence of heterogeneous phases with significant improvement in electrical and magnetoelectric properties of BaFe<sub>12</sub>O<sub>19</sub>/BiFeO<sub>3</sub> multiferroic ceramic composites, *Ceram. Int.* 45 (2019) 22889–22898.
- [8]. A. Jain, Y.G. Wang, N. Wang, Y. Li, F.L. Wang, Tuning the dielectric, ferroelectric and electromechanical properties of Ba<sub>0.83</sub>Ca<sub>0.10</sub>Sr<sub>0.07</sub>TiO<sub>3</sub>–MnFe<sub>2</sub>O<sub>4</sub> multiferroic composites, *Ceram. Int.* 46 (2020) 7576–7585.
- [9]. A. Jain, Y.G. Wang, N. Wang, Y. Li, F.L. Wang, Influence of individual phases on the magnetoelectric coupling and electromechanical response in (1-x) Ba<sub>0.83</sub>Ca<sub>0.10</sub>Sr<sub>0.07</sub>TiO<sub>3</sub>-xBiFeO<sub>3</sub> (x = 0–0.30) multiferroic composites, *J. Magn. Mater.* 495 (2020).
- [10]. X. Tan, C. Ma, J. Frederick, S. Beckman, K.G. Webber, The antiferroelectric ↔ ferroelectric phase transition in lead-containing and lead-free perovskite ceramics, *J. Am. Ceram. Soc.* 94 (2011) 4091–4107.
- [11]. Z. Liu, J. Lu, Y. Mao, P. Ren, H. Fan, Energy storage properties of NaNbO<sub>3</sub>-CaZrO<sub>3</sub> ceramics with coexistence of ferroelectric and antiferroelectric phases, *J. Eur. Ceram. Soc.* 38 (2018) 4939–4945.
- [12]. A. Jain, Y.G. Wang, N. Wang, Y. Li, F.L. Wang, Emergence of ferrimagnetism along with magnetoelectric coupling in Ba<sub>0.83</sub>Sr<sub>0.07</sub>Ca<sub>0.10</sub>TiO<sub>3</sub>/BaFe<sub>12</sub>O<sub>19</sub> multiferroic composites, *J. Alloys Compd.* 818 (2020).
- [13]. A. Jain, A.K. Panwar, Synergetic effect of rare-earths doping on the microstructural and electrical properties of Sr and Ca co-doped BaTiO<sub>3</sub> nanoparticles, *Ceram. Int.* 46 (2020) 10270–10278.
- [14]. G. Palareti, C. Legnani, B. Cosmi, E. Antonucci, N. Erba, D. Poli, S. Testa, A. Toso, Comparison between different D-Dimer cutoff values to assess the individual risk of recurrent venous thromboembolism: Analysis of results obtained in the DULCIS study, *Int. J. Lab. Hematol.* 38 (2016) 42–49.